Electric Field Redistribution due to Conductivity Changes during Tissue Electroporation: Experiments with a Simple Vegetal Model

A. Ivorra[1], L.M. Mir[2,3] and B. Rubinsky[1,4]

[1] Depts. of Mechanical Eng. and Bioengineering, University of California at Berkeley, Berkeley, CA, USA
[2] UMR 8121 CNRS-Institut Gustave-Roussy, Villejuif, France
[3] Univ. Paris-Sud, UMR 8121
[4] Center for Bioengineering in the Service of Humanity and Society, Hebrew University of Jerusalem, Jerusalem, Israel

Abstract— **Electroporation, or electropermeabilization, is the phenomenon in which cell membrane permeability to ions and macromolecules is increased by exposing the cell to short high electric field pulses. In living tissues, such permeabilization boost can be used in order to enhance the penetration of drugs (electrochemotherapy) or DNA plasmids (electrogenetherapy) or to destroy undesirable cells (irreversible electroporation). During the application of the high voltage pulses required for *in vivo* electroporation treatments, the conductivity of the involved tissues increases due to the electroporation phenomenon. This alteration results in a redistribution of the electric field magnitude that should be taken into account at treatment planning in order to foresee the areas that will be treated by electroporation. In the last five years some authors have indeed started to include such conductivity alteration in their simulation models. However, little experimental evidence has been provided to support the fact that conductivity changes really have a significant role on the electric field distribution. By reporting experiments on potato tuber, here we show that conductivity increase due to electroporation has indeed a significant physiological effect on the result of the application of the pulses. For instance, we noticed that by taking into account such conductivity alteration during simulations the error in electroporated area estimation went down from 30 % to 3 % in a case in which electroporation was performed with two parallel needles. Furthermore we also show that the field redistribution process occurs in two stages: an immediate and fast (<5 μs) redistribution after the pulse onset, probably only held up by the cell membrane charging process, and a slower, and less significant, redistribution afterwards probably related to slow, and moderate, changes in tissue conductivity during the pulse.**

Keywords— **Electroporation, Tissue Conductivity, Electric Field, Potato, Finite Element Method.**

I. Introduction

Electroporation, or electropermeabilization, is the phenomenon in which cell membrane permeability to ions and macromolecules is increased by exposing the cell to short (microsecond to millisecond) high electric field pulses. Reversible electroporation of living tissues is the basis for different therapeutic maneuvers on clinical use or under study [1] such as the in vivo introduction of genes into cells (electrogenetherapy) and the introduction of anti-cancer drugs into undesirable cells (electrochemotherapy). More recently, irreversible electroporation (IRE) has also found a use in tissues as a minimally invasive surgical procedure to ablate undesirable tissue without the use of adjuvant agents [2-4].

Electroporation is a dynamic phenomenon that depends on the local transmembrane voltage. It is generally accepted that, for a given pulse duration and shape, a specific transmembrane voltage threshold exists for the manifestation of the electroporation phenomenon (from 0.5 V to 1 V). This leads to the definition of an electric field magnitude threshold for electroporation (E_{rev}); only the cells within areas where $|\mathbf{E}| > E_{rev}$ are electroporated. If a second threshold (E_{irrev}) is reached or surpassed, electroporation will compromise the viability of the cells because electroporation becomes irreversible (cells do not reseal). A larger threshold can also be defined ($E_{thermal}$) for the manifestation of thermal damage caused by the Joule effect. This is particularly relevant in the case of IRE ablation techniques: if irreversibility threshold is surpassed but thermal threshold is not reached then cells are destroyed but tissue scaffold is spared and that facilitates post-treatment healing [4].

For more than ten years [5] researchers have been employing numerical methods (e.g. the Finite Element Method (FEM)) for computing the electric field magnitude distribution and therefore for predicting the tissue volumes that will be effectively electroporated under a certain sample and electrode configuration. The most common model consists of one or multiple regions with constant electrical conductivities. Although this sort of models has been validated empirically with reasonably positive results [6, 7], recently it has been introduced a refinement [8, 9]: the electrical conductivity of the tissue is not constant but depends on the electric field magnitude it is experiencing. This feature models the fact that when electroporation occurs the conductivity increases abruptly and significantly. The conductivity increase results in a field redistribution which in turn results in a new conductivity redistribution and so on.

O. Dössel and W.C. Schlegel (Eds.): WC 2009, IFMBE Proceedings 25/XIII, pp. 59–62, 2009.
www.springerlink.com

Although this new refinement sounds perfectly logical, in our opinion, and to the best of our knowledge, no valid empirical evidence has been provided to support it against the more common and simpler models based on constant conductivities. It is precisely the purpose of the present study to provide evidences in this sense. It is also an objective of this paper to analyze how fast the field redistribution evolves.

Following the replacement concept of the 3 Rs approach for animal testing (**r**eduction of the number of animals, **r**efinement of procedures to reduce distress, and **r**eplacement of animal with non-animal techniques [10]), it is convenient to note here that some vegetables can be a proper alternative for studying bioelectrical aspects of tissue electroporation. In particular, raw potato tuber is a good choice because any irreversibly electroporated area will be distinctively darker about 5 hours after electroporation. Such darkening is probably due to an accelerated oxidation of chemical constituents caused by a decompartmentalization of certain enzymes and substrates [11] that occurs at cell lysis caused by electroporation. Here we have chosen to wait for 12 hours before observing the effects of the high voltage pulses.

II. Methods

A. Uniform field electroporation

Sixteen potato tuber cylinders of 5 mm in diameter and approximately 5 mm in height were electroporated between two large plate electrodes made of aluminum (Fig 1.a) attached to a dielectric digital caliper (Digimatic by Mitutoyo Corp., Kawasaki, Japan) for accurate assessment of cylinder height. The electroporation protocol consisted of a single pulse of 400 µs. Multiple voltages, ranging from 50 V to 500V, were selected in the electroporation generator (ECM 830 by BTX-Harvard Apparatus Inc., Holliston, MA, USA). Voltage and current waveforms were recorded with a digital oscilloscope (WaveRunner 44Xi by LeCroy Corp., Chestnut Ridge, NY, USA).

This electrode and sample configuration produces a uniform electric field magnitude distribution ($|\mathbf{E}|=\Delta V/d$), without edge effects, if the sample is homogeneous.

After the electroporation pulse, the samples were kept in Petri dishes (for minimizing dehydration) for 12 hours at room temperature. Then a single picture of all the samples on a white sheet was taken with a digital camera (C-7070 by Olympus Corp., Tokyo, Japan). The obtained color image was converted to a grayscale image and brightness and contrast were adjusted (software Photoshop 8.0 by Adobe Systems Inc., Mountain View, CA, USA) so that the white paper had a 0% black content ("K"), the non treated potato cylinder had a K of about 60% and the darkest cylinders ($|\mathbf{E}| > 800$ V/cm) had a K of about 95%. The black content of the samples was represented against the electric field magnitude each one of them experienced (Fig 1.c) and a linear piecewise function was obtained for the relationship between K and $|\mathbf{E}|$.

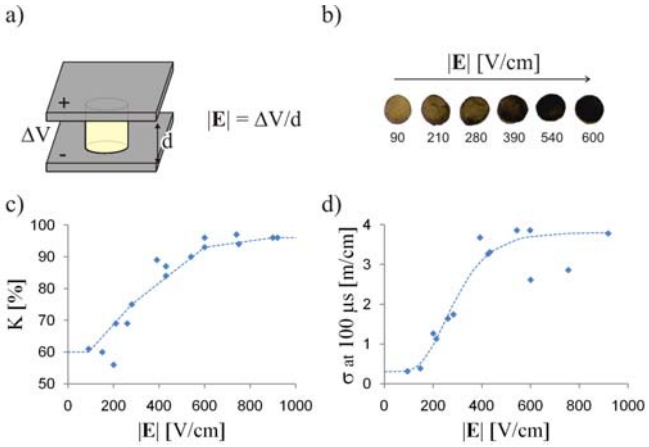

Fig. 1 a) Potato tuber cylinders are electroporated between two large plates. b) After 12 hours the cylinders exposed to higher fields are clearly darker. c) The "black contents" after 12 hours is represented against the field magnitude. d) Conductivity values at the 100th µs of the pulse and the sigmoid function used to model these values.

B. Ununiform field electroporation

A two needle electroporation array (5 mm separation, 0.3 mm in diameter, model 533 by BTX-Harvard Apparatus Inc., Holliston, MA, USA) was inserted across the center of a rectangular piece (20 mm × 20 mm × 5 mm) of potato tuber (similarly to what is shown in Fig. 2). Then a single pulse of 400 µs and 300 V was applied with the ECM 830. The same process was repeated with a 500 V pulse.

Both pieces were kept in Petri dishes for 12 hours and pictures were obtained and processed as it is described in the previous subsection (result images are subfigures a and b of Fig 3; only the central 15 mm × 15 mm section is displayed).

C. Finite Element Method simulations

Bidimensional FEM simulations of a model equivalent to the case described in subsection B were performed with COMSOL Multiphysics 3.4 (Comsol AB, Stockholm, Sweden). A very similar simulation process is described in [9].

Two conductivity models for the potato tissue were considered here: 1) constant conductivity ($\sigma(|\mathbf{E}|)=0.3$ mS/cm) and 2) conductivity according to the values obtained at the

100^{th} μs of the pulse (Fig 1.d), which are approximated with the following sigmoid function (fitted automatically with the *Curve Fitting Toolbox* of Matlab 7.6 by The Mathworks, Inc., Natick, MA, USA):

$$\sigma(|\mathbf{E}|) = 3.5\, e^{-e^{-0.01(|\mathbf{E}|-250)}} + 0.3 \quad [\text{mS/cm}] \qquad (1)$$

In the second conductivity model, field dependent, the simulation was solved as an iterative process with a sequence of steps in which the conductivity for each step was defined by the field in the previous step.

The simulated electric field magnitude was then displayed with the gray scale obtained with the samples of subsection A (Fig. 1.c)

D. Voltage recordings for assessing redistribution speed

From the above referred simulation at 500 V with field dependent conductivity, two points were selected (Fig. 2): p1) a point in which the potential is constant (ΔV/2= 250 V) across all the simulation steps and p2) a point in which there is a significant difference between the voltage at the first step, $V_{STEP\ 0}$ (i.e. before conductivity has been modified according to electric field magnitude), and the voltage at the step in which a stable solution has been reached, $V_{STEP\ \infty}$.

In principle, immediately after the onset of the pulse, the recorded potential at p2 should be equal to $V_{STEP\ 0}$ whereas after the whole redistribution process is finished it should be equal to $V_{STEP\ \infty}$.

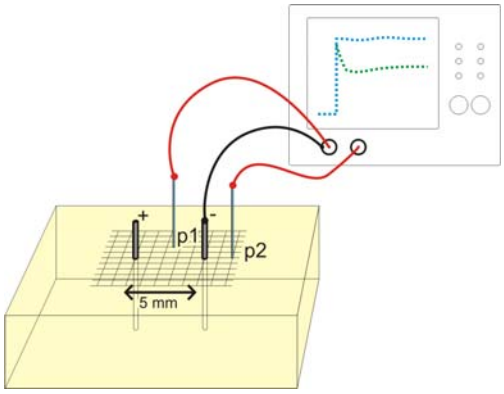

Fig. 2 Voltage recordings (at points p1 and p2) for analyzing the dynamics of electric field redistribution. A 500V and 400μs pulse is applied between the needle electrodes + and -. Recording electrodes at p1 and p2 are stainless steel hypodermic needles (diameter = 0.28 mm).

III. Results and Discussion

A. Uniform field electroporation

See Fig. 1.

B. Comparison of simulation results and electroporated areas according to conductivity models

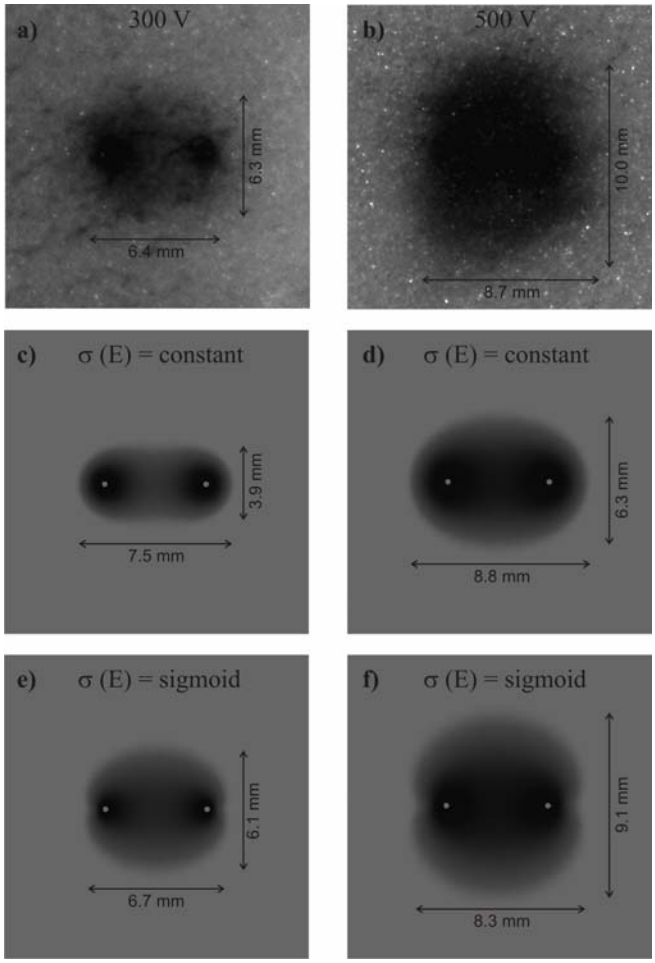

Fig. 3 a) Processed black and white picture (brightness and contrast adjustment) of a potato tuber slice 12 hours after electroporation with two parallel needles at 300 V(separation = 5 mm). b) the same with ΔV= 500V. c) and e) simulation of the 300 V case with constant conductivity (c) and with field dependent conductivity according to eq. 1 (e). d) and f) the same than e and f but for the case ΔV= 500V. The area represented in all the subfigures is a 15 mm × 15 mm section.

Fig. 3 shows that by including the dependence of the conductivity on the field the simulations are indeed closer to the actual effect of the pulses. With the aid of Engauge Digitizer (http://digitizer.sourceforge.net) we computed the

electroporated areas for all the subfigures shown in Fig. 3: a) 33 mm^2, b) 83 mm^2, c) 23 mm^2, d) 45 mm^2, e) 32 mm^2 and f) 62 mm^2. Therefore, by including the conductivity dependence effect, the area error for the 300 V case goes down from 30% to 3% whereas for the 500 V case the area error goes down from 46 % to 25 %.

Here it is necessary to note that potato tuber is a special case of biological tissue in the sense that its extracellular conductivity is exceptionally lower than its intracellular conductivity and that induces a huge increase of conductivity when electroporation occurs (approx. ×12 in Fig. 2.d). Soft animal tissues only augment their conductivity during electroporation pulses in ×3 to ×6 factors [12-14]. Therefore, in those cases the effect of the conductivity dependence on the electric field should not have such significant consequences as the ones displayed in Fig. 3.

C. Dynamics of field magnitude redistribution

In Fig. 4 it can observed that, as expected, voltage at point p1 is almost constant during the first quarter of the pulse and almost equal to $\Delta V/2 = 250$ V (error is probably caused due to location inaccuracy). However, voltage at p2 seems to show that the field redistribution behaves as a two stage process: an immediate and fast (<5 µs) phase after the pulse onset in which the voltage drops almost 50 V (as expected by the difference between $V_{STEP\ 0}$ and $V_{STEP\ \infty}$), probably only held up by the cell membrane charging process, and a slower, and less significant, redistribution phase afterwards probably related to slow, and moderate, changes in tissue conductivity during the pulse; note that the simulated $V_{STEP\ \infty}$ was obtained with conductivity values at 100 µs but that the conductivity of the uniform field samples increased moderately across the pulse (details not reported here due to space constrains).

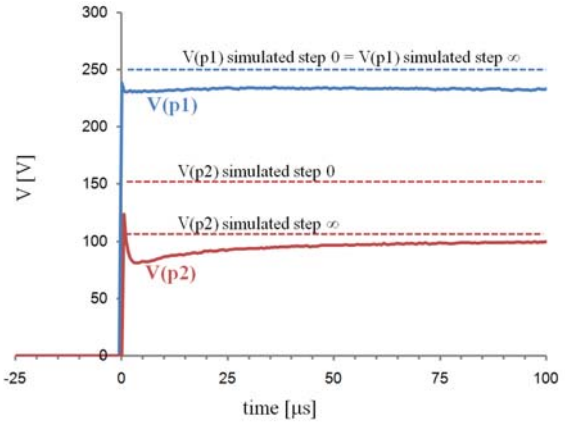

Fig. 4 Voltage recordings at points p1 and p2 during the first 100 µs of a 500 V pulse (see Fig. 1).

Acknowledgment

This work was supported in part by U.S. National Institutes of Health (NIH) under Grant NIH R01 RR018961.

BR has a financial interest in Excellin Life Sciences and Oncobionic which are companies in the field of *in vitro* electroporation and *in vivo* IRE, respectively.

References

1. L. M. Mir, "Therapeutic perspectives of in vivo cell electropermeabilization," Bioelectrochemistry, vol. 53, pp. 1-10, 2000.
2. R. V. Davalos, L. M. Mir, and B. Rubinsky, "Tissue Ablation with Irreversible Electroporation," Ann. Biomed. Eng. , vol. 33, pp. 223, 2005.
3. B. Al-Sakere, F. André, C. Bernat, E. Connault, P. Opolon, R. V. Davalos, B. Rubinsky, and L. M. Mir, "Tumor ablation with irreversible electroporation," PLoS ONE, vol. 2, pp. e1135, 2007.
4. B. Rubinsky, "Irreversible electroporation in medicine," Technology in Cancer Research and Treatment, vol. 6, pp. 255-260, 2007.
5. D. Miklavcic, K. Beravs, D. Semrov, M. Cemazar, F. Demsar, and G. Sersa, "The Importance of Electric Field Distribution for Effective in Vivo Electroporation of Tissues," Biophys. J., vol. 74, pp. 2152-2158, 1998.
6. J. Edd, L. Horowitz, R. V. Davalos, L. M. Mir, and B. Rubinsky, "In-Vivo Results of a New Focal Tissue Ablation Technique: Irreversible Electroporation," IEEE Trans. Biomed. Eng. , vol. 53, pp. 1409-1415, 2006.
7. D. Miklavcic, D. Semrov, H. Mekid, and L. M. Mir, "A validated model of in vivo electric field distribution in tissues for electrochemotherapy and for DNA electrotransfer for gene therapy," Biochimica et Biophysica Acta, vol. 1523, pp. 73-83, 2000.
8. D. Sel, D. Cukjati, D. Batiuskaite, T. Slivnik, L. M. Mir, and D. Miklavcic, "Sequential finite element model of tissue electropermeabilization," IEEE Trans. Biomed. Eng., vol. 52, pp. 816-827, 2005.
9. A. Ivorra, B. Al-sakere, B. Rubinsky, and L. M. Mir, "Use of conductive gels for electric field homogenization increases the antitumor efficacy of electroporation therapies," Physics in Medicine and Biology, vol. 53, pp. 6605-6618, 2008.
10. W. M. S. Russell and R. L. Burch, The Principles of Humane Experimental Technique. London: Methuen & Co. Ltd., 1959.
11. I. N. A. Ashie and B. K. Simpson, "Application of high hydrostatic pressure to control enzyme related fresh seafood texture deterioration," Food Research International, vol. 29, pp. 569-575, 1996.
12. A. Ivorra and B. Rubinsky, "In vivo electrical impedance measurements during and after electroporation of rat liver," Bioelectrochemistry, vol. 70, pp. 287-295, 2007.
13. A. Ivorra, L. Miller, and B. Rubinsky, "Electrical impedance measurements during electroporation of rat liver and muscle," in 13th International Conference on Electrical Bioimpedance, vol. IFMBE Proceedings 17, H. Scharfetter and R. Merva, Eds. Berlin: Springer-Verlag, 2007, pp. 130-133.
14. D. Cukjati, D. Batiuskaite, F. Andre, D. Miklavcic, and L. M. Mir, "Real time electroporation control for accurate and safe in vivo non-viral gene therapy," Bioelectrochemistry, vol. 70, pp. 501-507, 2007.

Author: Antoni Ivorra
Institute: University of California at Berkeley
Street: 6124A Etcheverry Hall
City: Berkeley, CA 94720
Country: USA
Email: antoni.ivorra@gmail.com